




Structure-guided design and evaluation of CRM197-scaffolded vaccine targeting GnRH for animal immunocastration

Yurong Duan^{1,2} · Xiaowen Tang³ · Sha Liu¹ · Weiwei Cui¹ · Mengge Li⁴ · Shiyu tang¹ · Wenrong Yao⁶ · Wenjie Li¹ · Jiachen Weng¹ · Junjie Zhao¹ · Zhun Wei^{1,2,5} 

Received: 30 January 2024 / Revised: 23 October 2024 / Accepted: 28 October 2024
© The Author(s) 2024

Abstract

Immunocastration is a humane alternative to surgical castration for controlling population and estrous behaviors in animals. Gonadotropin-releasing hormone (GnRH), the pivotal initiating hormone of the hormonal cascade in mammals, is the optimal target for immunocastration vaccine development. Cognate antigen-mediated cross-linking of B cell receptors (BCRs) is a strong activation signal for B cells and is facilitated by repetitive surface organizations of antigens. In this study, we describe the structure-guided design of highly immunogenic chimeric proteins with variant numbers of GnRH peptide insertion by epitope grafting. Linear B-cell epitopes of cross-reacting material 197 (CRM197) were replaced with multiple copies of GnRH peptide, and the inserts were displayed on the surface of the designs while maintaining the overall folding of CRM197. Among the seven designs, TCG13, which carries 13 copies of GnRH peptide, was the most immunogenic, and its immunocastration efficacy was evaluated in male mice. Vaccination with the BFA03-adjuvanted TCG13 induced potent humoral immunity and reduced the serum testosterone concentration in mice. It could significantly decrease sperm quality and severely impair gonadal function and fertility. These results demonstrate that CRM197 holds great value as a scaffold for epitope presentation in peptide-based vaccine development and supports TCG13 as a promising vaccine candidate for animal immunocastration.

Key points

- Provide a feasible way to design chimeric immunogen targeting GnRH by epitope grafting.
- CRM197 can accommodate the insertion of multiple copies of heterologous epitope peptides.
- Administration with the most immunogenic design led to effective immunocastration in male mice.

Keywords Immunocastration vaccine · Epitope grafting · CRM197 · GnRH · Chimeric antigen

Yurong Duan and Xiaowen Tang contributed equally to this work.

✉ Zhun Wei
biowei@qdu.edu.cn

¹ Department of Pharmacology, School of Pharmacy, Qingdao University, Qingdao 266073, China

² Institute of Innovative Drugs, Qingdao University, Qingdao 266021, China

³ Department of Medical Chemistry, School of Pharmacy, Qingdao University, Qingdao 266073, China

⁴ School of Stomatology, Qingdao University, Qingdao 266003, China

⁵ Keynova Biotech Co, Ltd, Weifang 261071, China

⁶ Jiangsu Recbio Technology Co., Ltd, Taizhou 225300, China

Introduction

Immunocastration is a humane alternative to surgical castration for controlling the population of various animals (wild, zoo, farm, and domestic) (Gupta and Minhas 2017; Kim et al. 2019; Naz and Saver 2016). It is also useful in the management of undesirable behaviors of zoo and domestic animals. Gonadotropin-releasing hormone (GnRH), the central initiator of the reproductive hormonal cascade, is an excellent immunocastration target for animals of sexes. GnRH affects the reproductivity of both male and female; antibodies generated by immunization against GnRH prevent circulating GnRH from binding to pituitary receptors and therefore block the release of follicle-stimulating hormone (FSH) and luteinizing hormone (LH) and subsequently lead

to atrophy of the gonads and infertility in both genders (Ein-
arsson et al. 2011; Millar 2005; Whitlock et al. 2019).

Traditionally, for the production of a GnRH vaccine, the non-immunogenic GnRH decapeptide requires chemical conjugation to a potent immunogenic carrier protein due to the lack of CD4⁺ response (Dalum et al. 1997). Up to now, all licensed GnRH vaccines on the market are conjugate vaccines (Naz and Saver 2016; Khumsap et al. 2024; Ochoa et al. 2023). However, conjugate vaccines are often associated with poor homogeneity and complicated preparation methodologies due to chemical conjugation reactions. To overcome the inherent disadvantages of GnRH conjugate vaccines, a variety of approaches have been applied to prepare well-defined GnRH subunit vaccines with enhanced immunogenicity. These efforts shed light on the development of the next-generation GnRH vaccine. A tandem repeated GnRH-I hexamer fused to maltose-binding protein (MBP) expressed in *Escherichia coli* showed high immunogenicity with improved homogeneity (Fang et al. 2010; Jiang et al. 2015). A tandem repeat of the GnRH primary sequence fused with the non-pathogen-associated linker sequence was designed, and a long-lasting specific immune response against GnRH and high anti-GnRH antibody titers was detected in both male and female BALB/c mice immunized upon immunization (Siel et al. 2016, 2024). In a more recent study, a recombinant fusion protein containing eight repeats of GnRH-I plus four T-helper epitopes was demonstrated to be effective in terms of reducing fertility in mice and dogs (Chang et al. 2021, 2023).

B-cell activation is pivotal for the subsequent immune responses, and it is initiated by the binding of cognate antigen to the B cell receptor (BCR) (Liu and Chen 2005). Several variables such as size, density or valency, and surface properties of an antigen are critical for the efficient activation of B-cells and secretion of antibodies (Pone et al. 2022; Wen et al. 2019; Zeigler et al. 2019). Owing to the advances in structural biology, in particular, computational biology, these parameters can be tailored to guide the design of antigens with improved immunogenicity.

Here, we presented a feasible way to design a novel GnRH vaccine immunogen by grafting GnRH peptide into Cross-reactive material 197 (CRM197) aided by computational design. CRM197 is the diphtheria toxin (DT) non-toxic mutant successfully used in many polysaccharide conjugate vaccines (Conde et al. 2021; Giannini et al. 1984; Malito et al. 2012; Pichichero 2013), and its immune-stimulant properties as a carrier protein has been employed in subunit vaccine development (Bellone et al. 2021; Wang et al. 2019). Recently, a synthetic tandem-repeated GnRH hexamer (GnRH6) fused to CRM197 was prepared, and its efficacy was proved in male rats (Gong et al. 2024). Carrier-induced epitope suppression (CIES) was a phenomenon wherein antibodies produced in response to peptide

conjugate vaccines and polysaccharide vaccines may hinder the subsequent immune response elicited by the same vaccine (Dalum et al. 1997). Although the precise mechanisms underlying CIES remains unclear to date, employing combinations of multiple vaccines utilizing different carriers has been shown to effectively mitigate certain instances of CIES (Pöllabauer et al. 2009; Xu et al. 2019). Instead of simply transplanting the GnRH peptide into CRM197, we replaced several linear B-cell epitopes of CRM197 with multiple copies of the GnRH peptide, thus increasing the density of GnRH on the chimeric molecule while reducing the possible CIES effect. To enhance the size and solubility of the designed antigen, *E. coli* trigger factor (TF) was fused to the N terminus of each design (Ferbitz et al. 2004; Hoffmann et al. 2010; Wu et al. 2022).

Based on the aforementioned strategy, seven CRM197-GnRH chimeric antigens with variable GnRH insertions were designed and expressed in *E. coli* followed by purification. The immunogenicity of all the antigens was firstly evaluated in female BALB/c mice, and the antigen that elicited the highest anti-GnRH antibody titers was then systematically investigated for immunocastration efficacy in male BALB/c mice (Fig. 1). This new GnRH vaccine antigen was proved to be safe, highly immunogenic, and able to reduce gonadal function, as well as fertility in the administered mice. This method eliminates conventional conjugation reactions and reduces the humoral response towards the carrier protein, which might reduce vaccine efficacy (Fig. 2).

Materials and methods

Structure-guided design of the CRM197-GnRH chimeric antigens

CRM197 is a thermally and conformationally stable nontoxic form of DT that contains a single amino acid substitution from glycine to glutamate in position 52 (G52E) which still maintains the almost identical folding of DT. CRM197 protein sequence (GenBank accession number AMV91693.1) was acquired from NCBI and the three-dimensional structure of CRM197 (PDB ID: 4AE0) was obtained from the Protein Data Bank. The GnRH polypeptide (HWSYGLRPG) omitting the N-pGlu was used for peptide insertion (Ferro et al. 2002). Linear B-cell epitopes of DT have been recently identified (De-Simone et al. 2021). Chimeric antigens were designed by replacing linear B-cell epitopes located on the surface within non-structured regions of CRM197 with variant numbers of GnRH peptide. Molecular dynamic (MD) simulation was employed to evaluate the reliability of the designs.

The MD simulation was performed by using AMBER18 molecular simulation package (Lee et al. 2018). The Amber

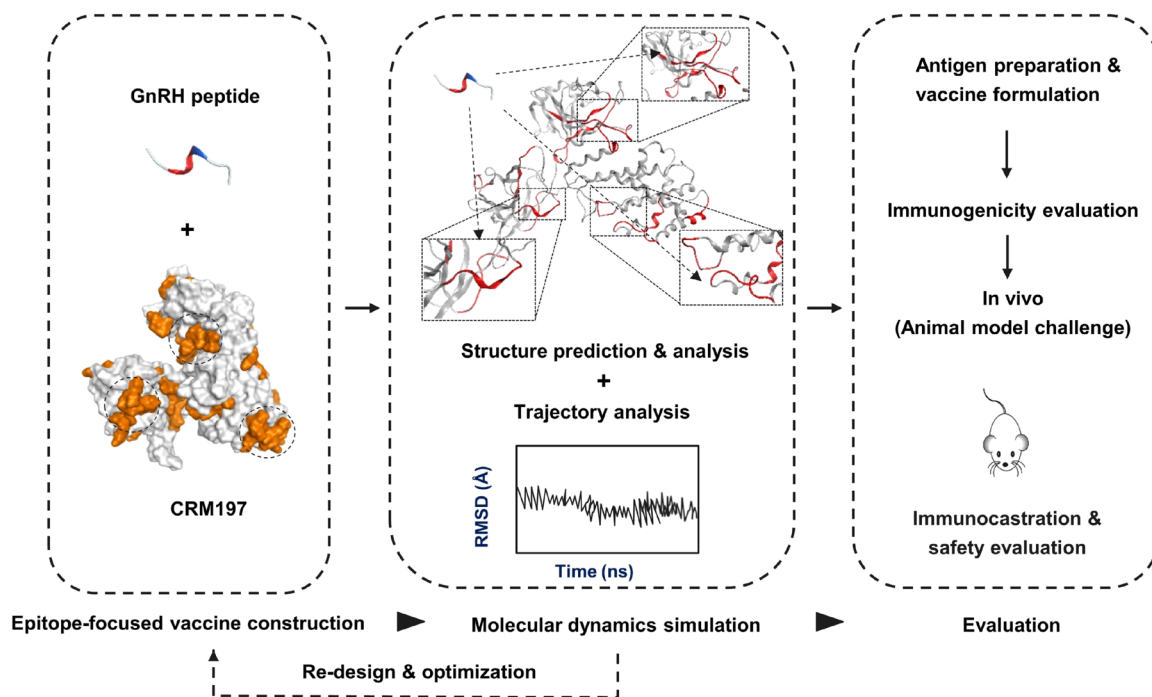


Fig. 1 Schematic representation of the designing and evaluation of an immunocastration vaccine candidate

ff14SB force field was employed for the proteins, and the TIP3P model was used for solvent water molecules (Alejandro et al. 1995; Maier et al. 2015). The initial coordinates and topology files were generated using the tleap program, incorporating neutralization and solvation. Subsequent classical MD simulations were executed within a cubic model under a periodic boundary condition. A series of routine minimization steps was conducted to relax the solvent and protein–ligand complex, first targeting solute atoms, then the protein backbone, and finally without constraint. Following the optimization, the system was gradually heated from 0 to 310 K over 100 ps under the NVT ensemble (N is number of particles, V is volume, T is temperature), followed by an additional 100 ps of MD simulations under NPT (N is number of particles, P is pressure, T is temperature) at 310 K and a target pressure of 1.0 atm. Subsequently, 250 ns NVT production MD simulations were performed at 310 K to obtain the trajectories. Throughout the simulations, the SHAKE algorithm was employed to constrain the high-frequency stretching vibration of all hydrogen-containing bonds, while a cut-off of 12 Å was established for both van der Waals (LJ-12 potential) and electrostatic interactions (PME strategy) (Jean-Paul Ryckaert and Berendsen 1977). The root mean square deviation (RMSD) and 3D protein structures extracted from the final MD trajectories were used to evaluate the reliability of modified proteins. By choosing the selected antigenic residues from the predicted 3D structure, it can be determined whether the GnRH peptide

epitope remains on the protein surface after replacement and whether the modified protein can still form a stable and complete protein structure.

Conjugate preparation, chimeric antigen expression, and purification

All the seven sequences encoding the designed CRM197-GnRH chimeric antigens were deposited in GenBank. These designs were CG1 (GenBank accession number PP271664), CG5c (GenBank accession number PP271665), CG8a (GenBank accession number PP271666), CG8b (GenBank accession number PP271667), CG10a (GenBank accession number PP271668), CG10c (GenBank accession number PP271669), and CG13 (GenBank accession number PP271670). The sequences were synthesized and cloned into the *Bam*HI/*Eco*RI sites of the pCold-TFM expression vector (GENERAL Biosystems, Chuzhou, China), which was modified from the vector pCold-TF (Cao et al. 2016). Recombinant plasmids were transformed into *E. coli* BL21 (DE3) (Novagen, Darmstadt, Germany) competent cells and induced with 0.5 mM isopropyl-β-D-thiogalactoside (IPTG) (Solarbio, Beijing, China) at 16 °C for 16 h. Cultures were harvested by centrifugation and resuspended and lysed by a high-pressure cell crusher (Union-Biotech, Shanghai, China) in binding buffer (20 mM Na₂HPO₄/NaH₂PO₄, 500 mM NaCl, 5 mM imidazole, pH 8.0). After removing the insoluble cell portion by centrifugation at 48,000 × g for 30 min at

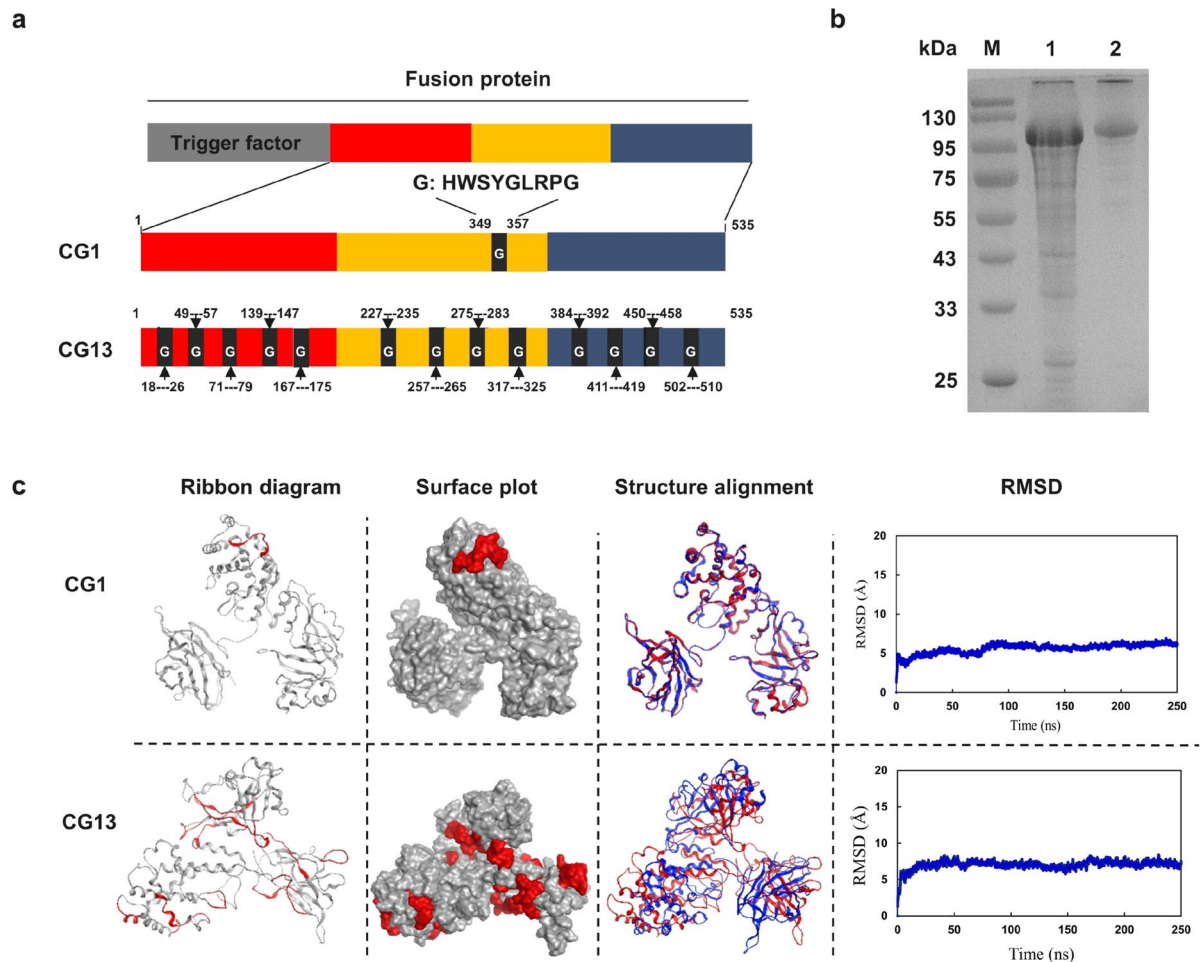


Fig. 2 Structure-guided design of the CRM197-GnRH chimeric antigens. **a** Schematic diagram of CG1 and CG13 antigen constructs. **b** Expression and purification of recombinant TCG13. Lane M: protein marker. Lane 1: supernatant. Lane 2: purified TCG13. **c** Bioinformatics analysis of CRM197-GnRH chimeric proteins based on the amino acid sequences. Three-dimensional models were obtained by mode-

ling and refinement. The relative locations of the polymorphic amino acid substitutions were shown on a surface plot. GnRH and CRM197-protein were shown in red and gray color, respectively. Structure superimposition of CRM197-GnRH chimeric antigens (red ribbon) and the monomer of wild-type CRM197 (PDB: 4AE0, blue ribbon). RMSD graphs for analyzing simulations of the trajectory (250 ns)

4 °C, the supernatant was loaded onto the Ni Sepharose 6 FF resin column (Cytiva, Marlborough, MA, USA) previously equilibrated with binding buffer. The resin was washed with 5 CVs (column volumes) washing buffer (binding buffer with 20 mM imidazole), followed by eluting with elution buffer (binding buffer with 250 mM imidazole). The eluent was changed to buffer A (20 mM NaHPO₄/NaH₂PO₄, 20 mM NaCl, 1 mM EDTA, pH 8.0) using a Desalting FF 5 mL column (Cytiva, Marlborough, USA) and then applied to a DEAE FF ion-exchange column (Cytiva, Marlborough, USA) in the Union-250 protein purification system (Union-Biotech, Shanghai, China). The target protein was collected in the flow-through fraction. Expressed and purified product of recombinant antigen was examined by 12% SDS-PAGE

analysis and quantified on a Nanodrop 2000 (ThermoFisher Scientific, Waltham, MA, USA).

To prepare the GnRH-CRM197 conjugates, the N-terminus of the primary GnRH sequence was modified by the addition of a cysteine (CHWSYGLRPG, Hefei KS-V Peptide Inc, China), which enabled conjugation with CRM197 (Keynova, Weifang, China) using sulfo-succinimidyl 4-[N-maleimidomethyl] cyclohexane-1-carboxylate (Sulfo-SMCC, Thermo Fisher Scientific, USA) according to the instructions in a two-step reaction scheme. The purified recombinant and final product were buffer changed into phosphate-buffered saline (PBS) and stored at -80 °C for vaccine preparation (final concentration of antigen was 2 mg/mL).

Antigen immunogenicity evaluation in BALB/c mice

Seven purified antigens were selected for immunogenicity evaluation; 30 µg of individual antigen was mixed with 50 µL BFA03 adjuvant kindly provided by Recbio Tech (Taizhou, China) for one dose. Healthy 7-week-old female BALB/c mice were purchased from HFK Bioscience (Beijing, China) and maintained according to the local animal care guidelines in the Animal Care Unit of Qingdao University (Qingdao, China). Manipulations involving animals were approved by the Qingdao University Laboratory Animal Welfare Ethics Committee (Approval No.20220507BALB/c4020220823002). Forty 8-week-old female BALB/c mice were randomly divided into eight groups ($n=5$), and each group was subcutaneously vaccinated twice at 2-week intervals. Blood samples were collected via tail bleeding at week 6. Samples were centrifuged at 4000 r/min for 20 min. The serum was collected and stored at $-80\text{ }^{\circ}\text{C}$ for future use in antibody measurements.

To compare the immunogenicity of GnRH-CRM197 conjugates and TCG13, ten eight-week-old female BALB/c mice were purchased and maintained as mentioned above (Approval No. 20240808BALB/c1020240921011). All the mice were randomly divided into GnRH-CRM197 conjugates group (30 µg, $n=5$) and TCG13 group (30 µg, $n=5$). Immunization procedure was as described above. Blood samples were collected at week 6 and processed for antibody measurements.

Immunological castration evaluation in male BALB/c mice

Healthy 7-week-old male BALB/c mice were purchased and maintained as mentioned above (Approval No. 20220921BALB/c3020230311003). Thirty 8-week-old male BALB/c mice were randomly divided into five groups ($n=6$); the immunization schedule is shown in Fig. 3a. Each group was subcutaneously vaccinated with PBS, CRM197 (30 µg, Keynova Biotech, Weifang, China), TF (30 µg,

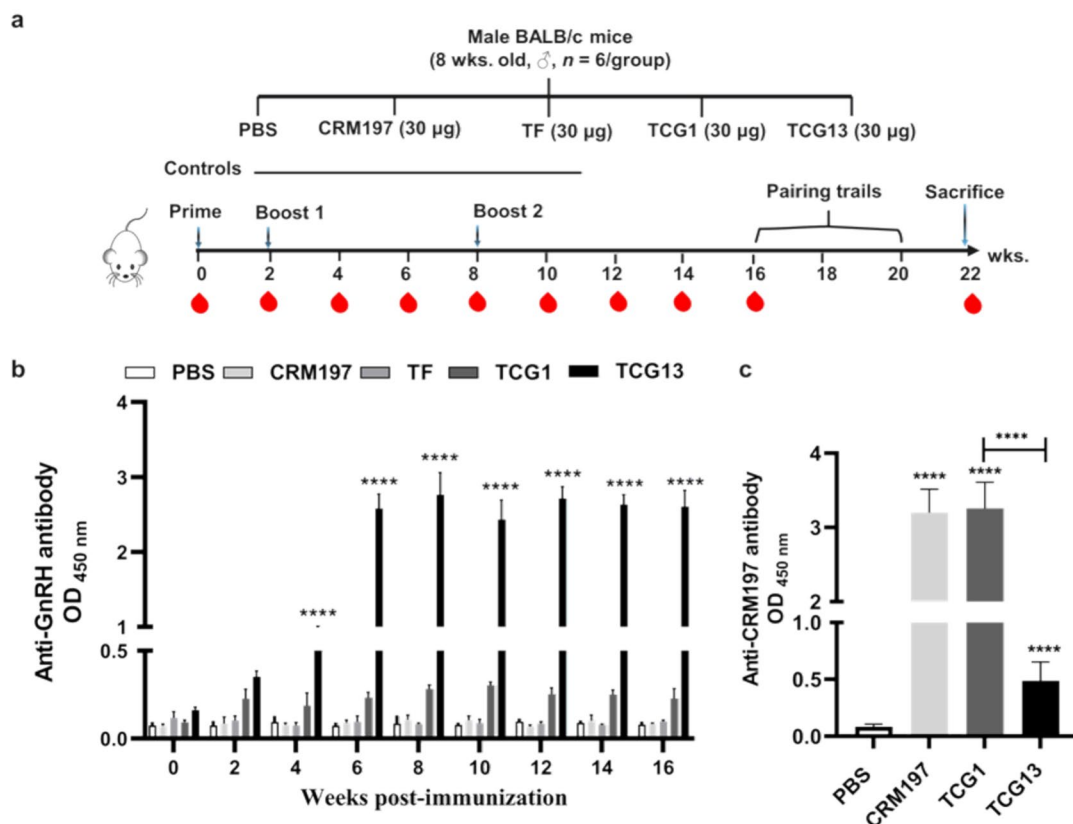


Fig. 3 Humoral immune response triggered by vaccination. **a** Vaccination and sampling schedule. Male mice were vaccinated with TCG1 or TCG13 (PBS, CRM197 or TF as controls) formulated with BFA03 adjuvant, respectively. **b** ELISA analysis of anti-GnRH IgG levels (1:5000 serum dilution) of the vaccinated and control groups

from week 0 to week 16. **c** The levels of anti-CRM197 IgG at week 8 (1:10000 serum dilution). Statistical analysis was performed using one-way ANOVA followed by the Tukey test. All results were expressed as mean \pm SD ($n=6$); **** $P<0.0001$ compared with the PBS group. Samples were analyzed in triplicate

prepared in our lab), TCG1 (30 µg), or TCG13 (30 µg), formulated with 50 µL of BFA03 adjuvant at week 0, 2, and 8, respectively.

Sample collection

The blood samples (150 µL) were collected at 2-week intervals via the jugular vein from each mouse at 7:00–8:00 am due to the diurnal variation. All the samples were processed as mentioned above. At study week 22, all the mice were anesthetized with 4% isoflurane and sacrificed by cervical dislocation. The bilateral testes/epididymides, heart, liver, spleen, lung, and kidney were dissected and weighed from each mouse. The testis and the left epididymis of each mouse were fixed with Davidson's solution for 24 h at room temperature. The right epididymis was preserved in PBS for subsequent sperm quality assessment. Other organs were fixed in 4% paraformaldehyde. All organ samples were collected for hematoxylin–eosin (H&E, Solarbio, Beijing, China) staining as Jiang et al. (2015) described.

Detection of specific antibodies

GnRH-BSA conjugates (coating antigen) were prepared following the same procedure as that of GnRH-CRM197 conjugates. Serum anti-GnRH antibodies were detected using an enzyme-linked immunosorbent assay (ELISA), as previously described, with slight modifications (Chang et al. 2021). Briefly, GnRH-BSA conjugates (5.0 µg/mL, 0.05 M pH9.6 carbonate buffer) were coated onto the ELISA plate (100 µL/well, ThermoFisher Scientific, Waltham, MA, USA) overnight at 4 °C. After blocking using 5% (w/v) BSA (BSA, Sigma-Aldrich, St. Louis, MO, USA) for 3–4 h at room temperature, the diluted sera (1:5000) in PBS were added to the plate (100 µL/well) and incubated at 37 °C for 1 h. Goat anti-Mouse IgG/HRP (1:3000) was then distributed into each well for 1 h at 37 °C. The substrate TMB (3,3',5,5'-tetramethylbenzidine) was added and incubated at 37 °C for 10 min. The absorbance of each well was detected by a microplate reader at 450 nm.

The specific antibody responses against CRM197 were determined by ELISA similarly. Sera collected from the last booster injection were diluted to a 1/10,000 ratio using PBS.

Measurement of serum testosterone, FSH, and LH concentrations

Serum testosterone, FSH, and LH concentrations of male mice were measured using the commercial ELISA kits respectively (Jinma Biotech, Shanghai, China). Samples were assayed according to the manufacturer's instructions with each measurement carried out in duplicate, and each measurement was performed twice using the same ELISA

kit. Absorbance obtained was used to calculate the per reproductive hormone concentrations by interpolation with the respective standards.

Morphological observation of the testis and epididymis

After the execution, bilateral testes/epididymides were dissected for morphological measurement. Testis weight was recorded, and the length and width were measured using a vernier caliper. The formula for calculating testis volume was $V(\text{mm}^3) = 4/3\pi[\text{testis width}/2]^2[\text{testis length}/2]$. The testis coefficient was calculated with ratio = (testis volume/body weight).

Histological examination

Organs were fixed in 4% paraformaldehyde overnight before paraffin embedding, except for testes and the right epididymis, which were fixed in Davidson's solution (Solarbio, Beijing, China). Following fixation, organs were embedded in paraffin, serially sectioned at a thickness of 5 µm, then stained with H&E and observed under an inverted microscope for histopathological analysis of mice. The images were captured using a scanning microscope (Pannoramic MIDI, Budapest, Hungary) and analyzed using the SlideViewer 2.5 software (Pannoramic MIDI, Budapest, Hungary). Five seminiferous tubule diameters and epididymal tube diameters per mouse were randomly evaluated as described previously (Ulker et al. 2009).

Analysis of sperm quality

The epididymis was minced in PBS, and sperms were diffused for 20 min at 37 °C. The sperm suspension was used for subsequent analysis. Sperm parameters, including density, abnormality, and viability, were investigated according to the method previously described under a light microscope (Ochoa et al. 2023).

Mating test

Four-week-long mating test was arranged. Male mice were randomly caged with proven-breeder female mice in a 1:2 ratio from weeks 16–20. Female mice were examined for the presence of vaginal plugs every morning as evidence of mating since the pairing. If a plug was observed, the successfully mated mouse was housed individually. Offspring numbers were recorded and compared.

Statistical analysis

Data analysis and graphing were performed with GraphPad Prism software version 9 (GraphPad Software, San Diego, CA, USA). Data were expressed as mean \pm standard deviation (SD). Differences in results were analyzed using one-way ANOVA followed by Tukey post-tests among multiple groups or Student's *t*-test between two groups. Statistically significant differences were declared when $P < 0.05$ (* $P < 0.05$, ** $P < 0.01$, and *** $P < 0.001$, ns: not significant).

Results

Structure-guided design of the CRM197-GnRH chimeric antigens

In this study, CRM197-GnRH chimeric antigens were engineered, and representative designs (CG1 or CG13 which contains 1 or 13 copies of GnRH peptide insertion) are illustrated in Fig. 2a (other designs, Supplemental Fig. S1 and Fig. S2). To visualize the overall structure of the designed chimeric proteins, comparative models were built using the crystal structure of CRM197 (PDB ID: 4AE0) as a template. The RMSD of the main chain of the protein was calculated along the 250 ns MD simulation to predict the structural stability of the designs.

The RMSD value was an indispensable indicator of whether the system was converging or not, and also reflected whether the system had reached a steady state or not. For 250 ns simulations, trajectory analysis was performed. In Fig. 2c, the RMSD values of CG1 and CG13 arose at the outset and then continued to fluctuate. The relative locations of the replaced motif were shown on the surface plot of CG1/CG13. Interestingly, transplanted motifs were located on the surface of the simulated protein structure. Subsequently, the structure of the MD-simulated antigen was separately superposed with the original CRM197. Results showed that despite the movement of the spatial relative positions among the structural domains, the overall structure was still well-maintained. These designed antigens showed excellent foldability and indicated that CRM197 could serve as a scaffold for epitope grafting in vaccine development.

Expression, purification, and selection of antigen candidate

All seven designed CRM197-GnRH chimeric antigens expressed well in *E. coli* when fused to the TF tag. TF-fused CG1 was designated as TCG1 for abbreviation and other designs were named in the same manner. The fusion designs were purified through a two-step procedure. Analysis of the purified protein by 12% SDS-PAGE

revealed a dominant band of about 110 kDa corresponding to the estimated molecular weight of the chimeric proteins (theoretically ~59 kDa) plus the 6 \times His-TF tag (theoretically ~51 kDa) (Fig. 2b). Immunogenicity of the TF-fused designs was evaluated in female BALB/c mice by measurement of anti-GnRH IgG levels. It was found that the mice immunized with TCG13 have the highest level of anti-GnRH IgG. Not surprisingly, anti-GnRH IgG levels elicited by TCG1 were significantly lower than the other designs (Supplemental Fig. S3a). Then, TCG1 and TCG13 were selected for the study of immunological castration efficacy in male mice. Furthermore, we also compared the immunogenicity of GnRH-CRM197 conjugates and TCG13. While a high level of anti-GnRH antibodies was detected in the mice of GnRH-CRM197 conjugates group, the levels of anti-GnRH antibodies of the TCG13 group were higher than that of GnRH-CRM197 conjugates group detected at week 6 post-immunization (Supplemental Fig. S3b).

Anti-GnRH antibodies

To evaluate the humoral responses provoked by TCG1 or TCG13 in male mice, two kinds of specific antibodies were measured. Anti-GnRH antibody titers were detected by ELISA in male mice sera collected from weeks 0–16 at 2-week intervals. Results showed that the antibody titers against GnRH in TCG13 group were significantly increased from week 6 and maintained up to week 16 compared with the PBS group ($P < 0.001$) (Fig. 3b), suggesting TCG13 immunization induced an intense anti-GnRH immune response. All the animals treated with TCG13 developed a potent anti-GnRH response. TCG1 treatment elicited detectable levels of anti-GnRH IgG far below the TCG13 group, indicating that a single GnRH epitope grafting failed to induce a robust immune response. At the end of the experiment (week 22), anti-GnRH IgG levels of mice immunized with TCG13 remained at high levels (Supplemental Table. S4). Worthy of note, the levels of specific anti-CRM197 IgG were significantly lower than that of TCG1 group measured at week 8 post-immunization, while the TCG1 group had comparable levels of anti-CRM197 antibodies to the CRM197 group (Fig. 3c). These results clearly indicated that replacement of endogenous B-cell epitopes of CRM197 with multiple copies of GnRH peptide could substantially reduce the humoral response against CRM197 itself.

Serum testosterone, LH, and FSH concentrations

Serum testosterone (Fig. 4a), FSH (Fig. 4b), and LH (Fig. 4c) concentrations of male mice were measured by ELISA. At week 0, all the mice showed high serum testosterone, FSH, and LH levels, and no statistically significant difference was observed among the five groups

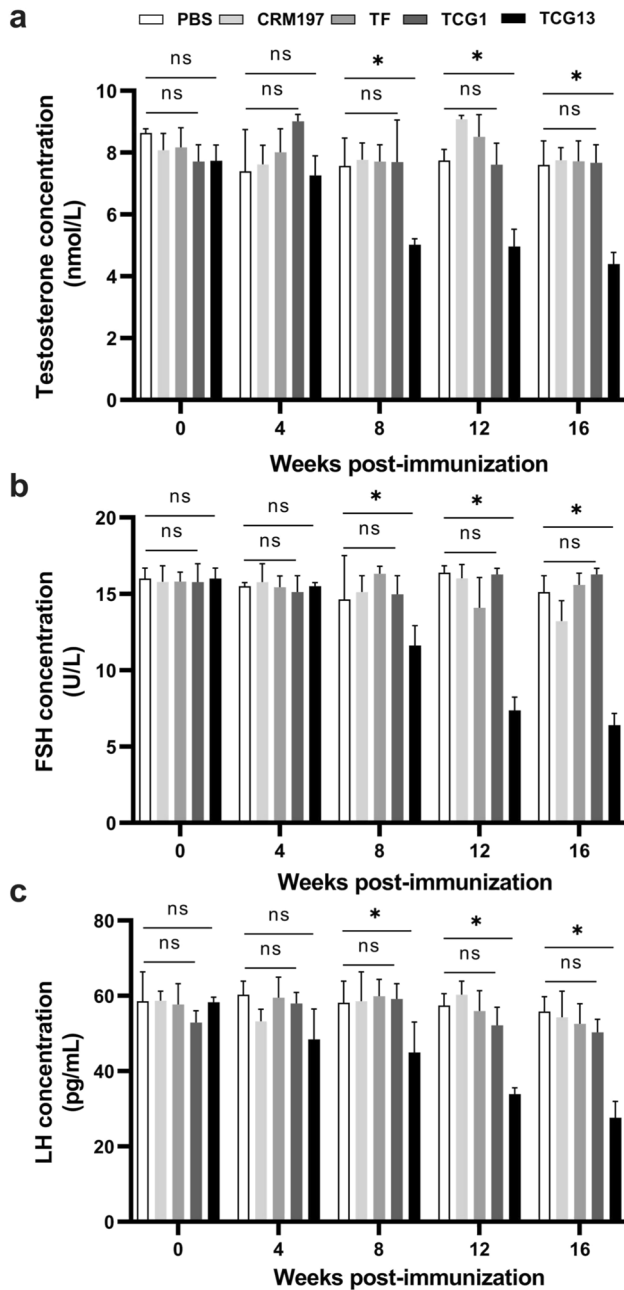


Fig. 4 Serum hormone levels in male mice. **a** Serum testosterone levels of male mice. **b** Serum FSH levels of male mice. **c** Serum LH levels of male mice. Hormone levels were monitored from week 0 to week 16 after primary immunization as indicated in the Fig. 3a. All results were expressed as mean \pm SD ($n=6$). * $P < 0.05$ compared with the PBS group. ns, not significant

($P > 0.05$). From week 8, serum testosterone, FSH and LH concentrations of the TCG13 group significantly reduced after the third immunization compared with the PBS group ($P < 0.05$), and the effects were maintained at week 16. As illustrated in Supplemental Table S4, the serum concentrations of testosterone (4.391 ± 0.84 nmol/L), FSH

(6.25 ± 1.13 U/L), and LH (32.472 ± 0.721 pg/mL) in mice immunized with TCG13 were still significantly lower than those in control groups at week 22. However, the TCG1 group had no statistical difference in serum testosterone, FSH, or LH concentrations compared with the PBS group. Collectively, these results clearly indicated that TCG13 immunization could substantially decrease serum testosterone, FSH, and LH concentrations in male mice.

Phenotypic analysis of the testis and epididymis

To further investigate the morphological changes of testis and epididymis, all mice were sacrificed at week 22. The results showed that, in contrast to the control groups (PBS, TF, CRM197) and TCG1 group, severe testicular atrophy was observed in TCG13 group (Fig. 5a). Also, testis weight (0.037 ± 0.003 vs. 0.099 ± 0.008 mg, $P < 0.0001$), volume (92.819 ± 25.787 vs. 187.147 ± 56.537 mm³, $P < 0.05$), and testis volume/body weight (4.150 ± 1.157 vs. 7.872 ± 2.922 , $P < 0.0001$) of TCG13-immunized mice were significantly reduced compared with PBS-immunized mice (Fig. 5b, c and Supplemental Table S1). Strikingly, compared with those in the PBS group, testis weight and size in the TCG13 group reduced by about 63% and 50%, respectively. Unsurprisingly, the epididymal length ($P < 0.05$) and weight ($P < 0.0001$) also showed a dramatic reduction in the TCG13 group compared with that of the PBS group.

Histological analysis of the testis

To evaluate histological changes of testis. H&E-stained sections of the testis were observed at 100 \times and 400 \times magnifications (Fig. 6). In PBS, CRM197, and TF groups, the layered and tightly arranged spermatocytes in different developmental phases of spermatogenesis in the testicular seminiferous tubules could be observed. On the contrary, the vacuolation of seminiferous tubules (vs. PBS group, $P < 0.0001$, Supplemental Table S1) and the absence of spermatogenesis were observed in testes of the TCG13 group. The severely damaged seminiferous tubules were evidenced by a substantial reduction in the number of mesenchymal stromal cells (yellow arrow). The testes of TCG13-immunized mice showed spermatogenesis caseation and the lumen with little or no spermatids and sperms (red arrow). However, the shape of the seminiferous tubules in the TCG1 group appeared normal, and there were different developmental stages of germ cells in the tubules and mature sperms in the lumen. Histopathological examination showed that TCG13 immunization caused severe testicular atrophy and impairment of spermatogenesis in mice (Fig. 6).

Fig. 5 Morphological observation of the testis in male mice at week 22 after primary immunization. **a** Testis photograph of all groups. **b** Comparison of testis weight. **c** Comparison of testis volume/body weight ratio. Statistical analysis was performed using one-way ANOVA test. All results were expressed as mean \pm SD ($n=6$). **** $P < 0.0001$ compared with the PBS group. ns, not significant

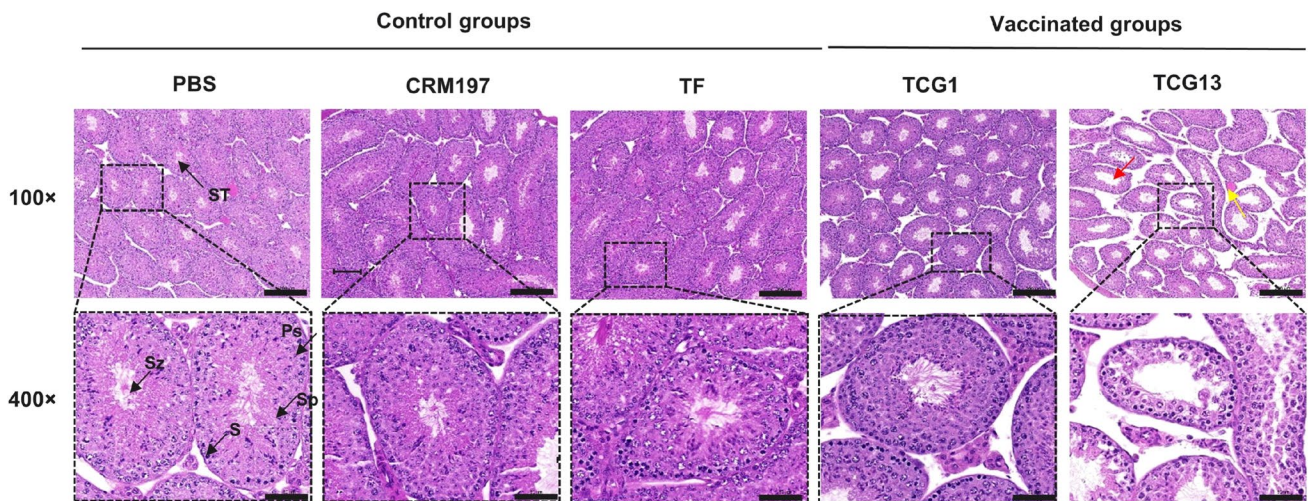
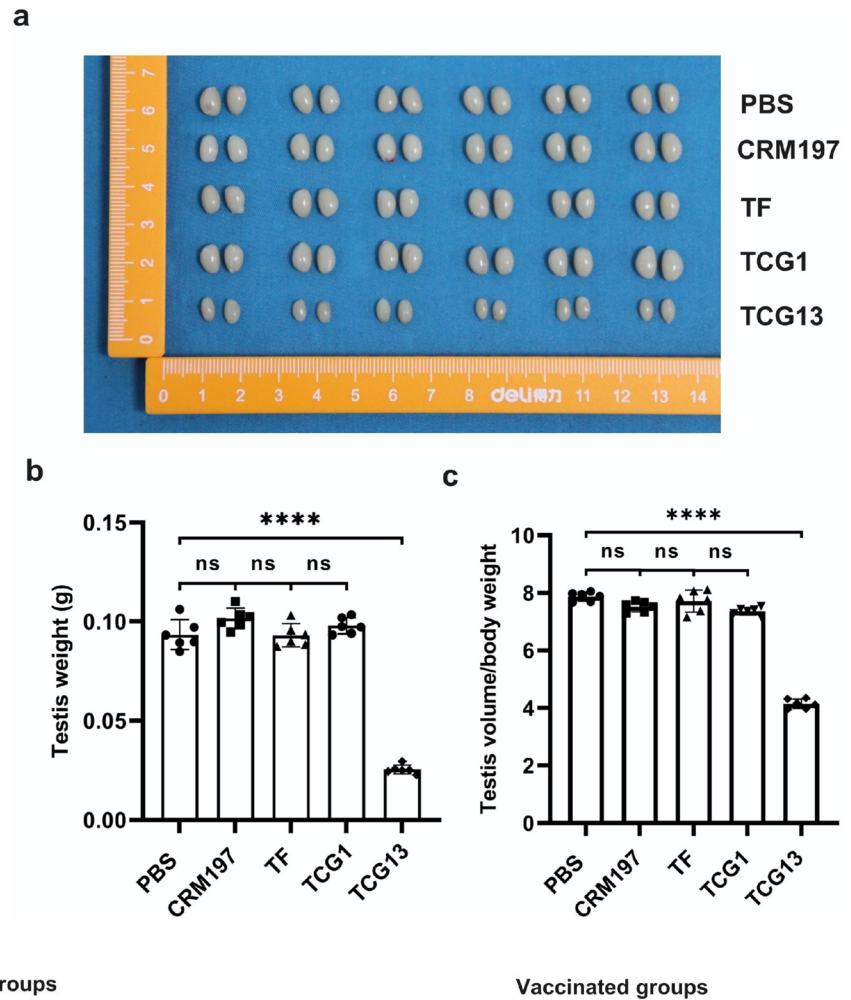


Fig. 6 Histological evaluation of the testis. Testis sections were stained by H&E from the control groups (PBS, CRM197, TF) and the vaccinated groups (TCG1, TCG13). Sections were observed at 100 \times and 400 \times magnifications. The seminiferous tubules (ST), spermatogonocytes (Sp), primary spermatocytes (PS), and spermatozoa

(Sz) are indicated with black arrows. The yellow arrow indicated multifocal germinal epithelium and Sertoli cell degeneration. The red arrow indicated seminiferous tubule degeneration. 400 \times images were enlarged schematic of the black boxed area in the 100 \times images. Scale bar: 200 μ m (100 \times) and 50 μ m (400 \times)

Histological analysis of the epididymis

Further analysis showed that the absence of spermatogenesis in the testis was paralleled by atrophy in the epididymis and seminal vesicles. The mice in the TCG13 group barely had sperms in the tubules (yellow arrow), and the epididymal duct lumen became smaller than the control groups (blue arrow, Fig. 7). The length of cilia on the surface of principal cells in the epididymal epithelium became shorter in mice immunized with TCG13. The average diameter of five random end-on epididymal ducts in the TCG13 group ($67.236 \pm 8.591 \mu\text{m}$) was statistically lower than PBS group ($130.376 \pm 16.073 \mu\text{m}$) (Supplemental Table S1). These effects were not observed in the epididymis of TCG1 group mice.

Sperm quality analysis

Sperm density, motility, and morphology were evaluated. Consistently, mice immunized with TCG13 exhibited decreased sperm quality parameters. Sperm density (Fig. 8a, $2.88 \pm 0.134 \times 10^5$ sperm/mL, $P < 0.0001$) and viability (Fig. 8c, $20.03\% \pm 7.84\%$, $P < 0.0001$) in TCG13 immunized mice decreased markedly compared with PBS group. Furthermore, the sperms concentrations in the three control groups were $3.04 \pm 0.724 \times 10^6$, $2.84 \pm 0.732 \times 10^6$, and $3.36 \pm 0.391 \times 10^6$ sperm/mL, respectively, which were not significantly different from those of the TCG1 group (Fig. 8a, $3.59 \pm 0.259 \times 10^6$ sperm/mL). The proportion of sperm abnormalities increased to $69.28\% \pm 12.22\%$ in the

TCG13 group (Fig. 8b). However, the TCG1 group did not show any significant change in sperm quality compared with the control groups.

Mating test

To investigate the fertility of immunized mice, all the mice cohabited with proven-fertility female mice for one month. Except for the number of pups per litter generated, we also recorded all mice exhibited mounting behavior during pairing stages. No pairing behavior was observed in the TCG13 group. Conception was not observed among the 12 female mice mated with the TCG13 group while all the mice became pregnant when mated with mice of the PBS group. The total number of pups among the five groups was 79, 70, 79, 75, and 0, respectively (Fig. 7d and Supplemental Table S2). No difference in the number of females producing litter or the proportion of mice that produced litter was found among the four groups except the TCG13 group (Fig. 7). Immunization with TCG1 did not significantly decrease the number of pups compared with the other controls.

Safety evaluation of recombinant GnRH vaccine

There was no significant difference in body weight among the five groups (Supplemental Fig. S4) and no deaths or inappropriate side-effects were observed. Also, no pathological changes were observed in the histological examination of major organs (Supplemental Table S3 and Fig. S5), indicating the safety of TCG13.

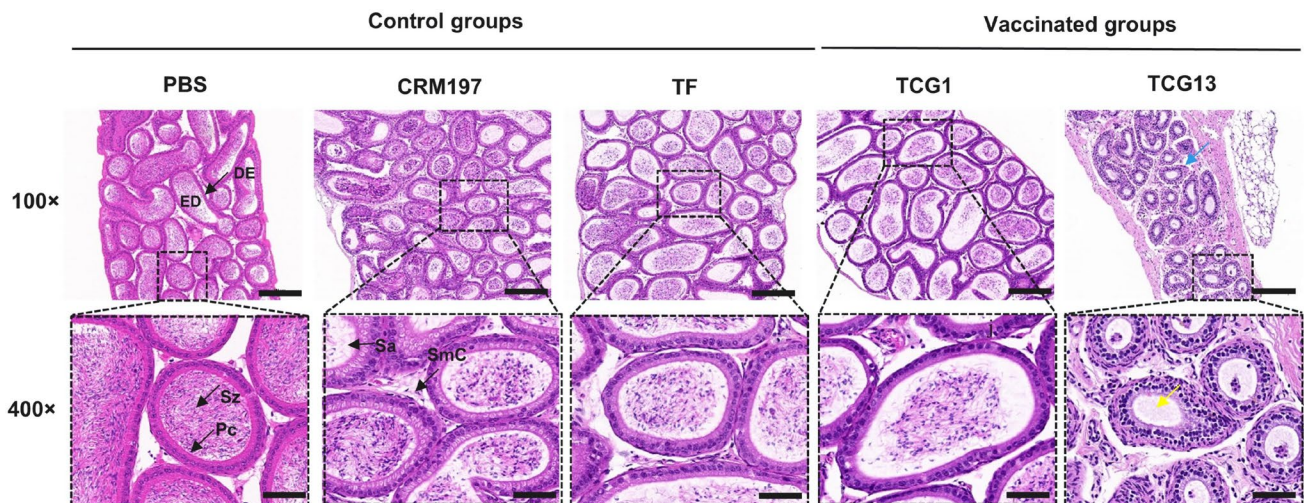
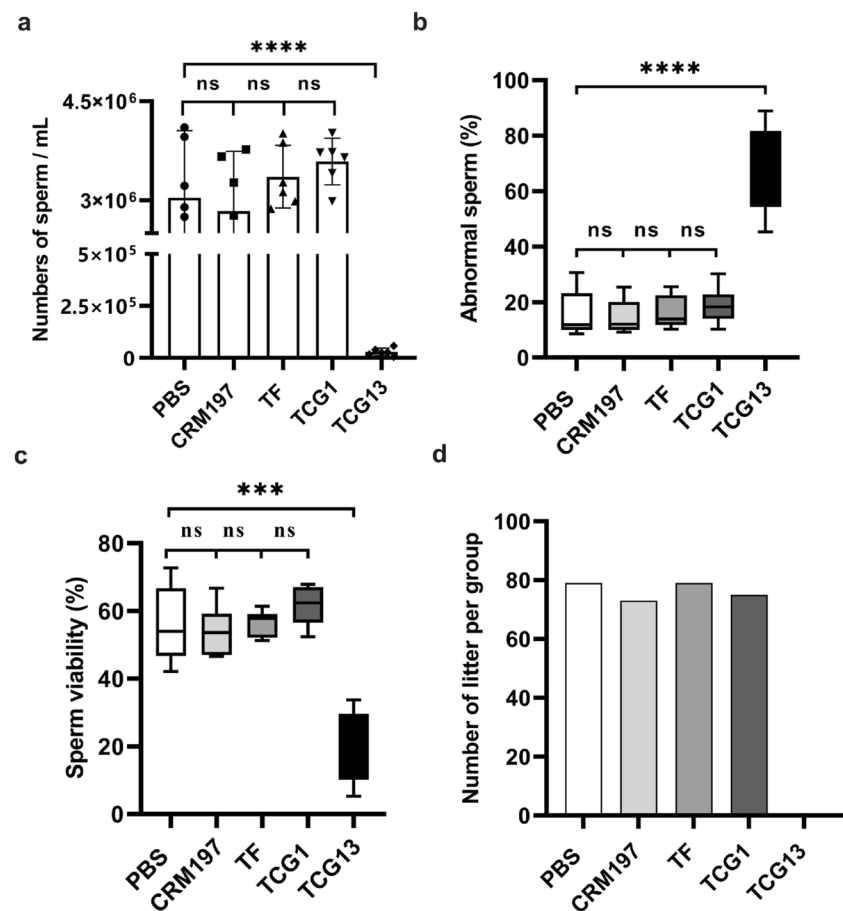


Fig. 7 Histological evaluation of epididymis. H&E-stained epididymis tissue sections were observed at 100 \times and 400 \times magnifications. The black arrows pointed to the epididymal epithelium (DE), smooth muscle cell (SmC), and static cilia (Sa). The increased epididymal space

(blue arrow) and absented sperms in the epididymal duct (ED, yellow arrow) of mice treated with TCG13. 400 \times images were enlarged schematic of the black boxed area in the 100 \times images. Scale bar: 200 μm (100 \times) and 50 μm (400 \times)

Fig. 8 Sperm quality and fertility test of immunized male mice. **a** Sperm concentration. **b** Percentage of abnormal sperms. **c** Sperm viability. Cauda epididymal sperms were taken from male mice at week 22 after primary immunization for sperm quality analysis. **d** Total numbers of litters from male mice each paired with two female mice between week 16 to week 20. Statistical analysis was performed using one-way ANOVA followed by the Tukey test. All results were expressed as mean \pm SD ($n=6$). **** $P < 0.0001$ compared with the PBS group. ns, not significant



Discussion

GnRH is the pivotal hypothalamic hormone regulating reproduction in mammals of both sexes and is widely conserved across all mammalian species. Thus, it makes it an ideal target antigen for immunocastration to control fertility and behavioral responses. As a small self-antigen, GnRH alone is of poor immunogenicity and the CD4⁺ T-cell epitope from a carrier protein is required to elicit anti-GnRH humoral response. Carrier conjugated GnRH vaccine has been successfully used in the controlling of boar taint which is related to testicular hormones and sexual maturity (Dunshea et al. 2001). For the population management of wildlife and domestic animals, single injection of the castration vaccine eliciting a long-lasting immune response and desired castrative efficacy is ideal, which requires the development of more potent immunogens and adjuvants as well as novel vaccine delivery platforms. Development of novel GnRH vaccines with improved homogeneity and immunogenicity remains demanding and challenging and there are ongoing efforts to improve the antigen delivery methods and rationally develop better adjuvants to improve immunogenicity.

Computational design of antigen is becoming a leading force of structural vaccinology, whereby protein is

engineered to display optimized immunological properties. In this context, epitope grafting, which entails the transplantation of an antibody recognition motif from one protein onto a different protein scaffold holds great promise for the design of superantigens (Azoitei et al. 2012; Correia et al. 2014; Vishweshwaraiah and Dokholyan 2022). Epitope grafting is particularly suitable for targeting linear peptides like GnRH as chemical conjugation with a carrier protein is avoided. Many studies have shown that the degree of repetitiveness of an antigen correlates with its efficiency in inducing a B-cell response and production of neutralizing antibodies (Liu and Chen 2005; Pone et al. 2022; Wen et al. 2019). Thus, rationally designed multivalent immunogens based on epitopes grafting approach might help to tackle the hurdles that lie in immunocastration vaccine development.

The objective of this study was to design a multivalent peptide-based immunogen targeting GnRH. In order to do so, CRM197 was used as a receptor scaffold for the insertion of multiple copies of GnRH peptides. CRM197 comprises three structurally independent domains termed catalytic (C, residues 1–187), transmembrane (T, residues 201–384), and receptor (R, residues 387–535) domains connected by an unstructured loop. The safety and high immunogenicity render CRM197 popular as one of the most widely used carrier

proteins for polysaccharide conjugate vaccines (Pichichero 2013). More importantly, the linear B-cell epitopes or segments of B-cell epitopes of DT have been elaborately characterized recently (De-Simone et al. 2021). We hypothesized that the structural properties and detailed B-cell epitope information of CRM197 make it amenable to the grafting of peptides to generate novel antigens.

In this study, the reported linear B-cell epitopes in the non-structured regions of CRM197 were selected as candidate sites for epitope replacement and variable numbers of GnRH peptides were transplanted. Surface exposure of the grafted peptides and the conformational stability of the designs were evaluated by the MD-simulation approach. Immunogenicity of the seven designs was preliminarily investigated in mice and all of the variants elicited strong antibody titers against GnRH except TCG1 which carries only one copy of GnRH peptide insertion. The TCG1 group showed only detectable antibody levels while the TCG13 group showed the highest antibody titer among all the tested designs. Another finding worthy of mention is that TCG13-induced anti-CRM197 humoral response was dramatically lower compared with TCG1 or CRM197 immunized group as most of the CRM197 B-cell epitopes in TCG13 were removed.

Then, immunocastration efficacy and safety of TCG13 were investigated in male mice, and TCG1 was included for comparison. TCG13 vaccinated mice showed potent GnRH-specific antibody titers, leading to substantially decreased serum testosterone, FSH, and LH concentrations; testicular atrophy; and reduced semen quality, concentration, morphology, and viability when compared with unvaccinated or TCG1 vaccinated mice. More importantly, the breeding capability of the TCG13 vaccinated mice was completely lost throughout the experimental period. These results clearly demonstrated that immunocastration efficacy upon vaccination is closely related to GnRH-specific antibody levels and TCG13 is a promising antigen for immunocastration.

The design described in this study has three obvious advantages over the conventional chemical conjugation approach, which usually involves the use of a heterologous carrier system to conjugate an antigen. Firstly, recombinant production of the designed antigen avoided the chemical conjugation procedures and improved the homogeneity of the product. Secondly, the incorporation of multiple copies of GnRH peptide increased the density of epitopes and substantially enhanced the humoral response against GnRH. Thirdly, replacement of the endogenous B-cell epitopes of CRM197 with GnRH peptide dramatically decreased the humoral immunity towards the carrier itself. It is plausible that the risk of CIES from booster vaccinations could be reduced in polysaccharide conjugate or peptide-based vaccines by substituting the carrier protein's dominant B-cell epitopes with exogenous peptides. Additionally, this study also clearly demonstrated that CRM197

can serve as a scaffold to accommodate the replacement of native B-cell linear epitope peptides with multiple exogenous epitope peptides while maintaining the structural integrity and immunogenicity as a carrier protein. The flexibility of the approach described here might be applicable to induce autoantibodies against other self-antigens like beta-amyloid plaques in Alzheimer's disease.

In conclusion, through the replacement of linear B-cell epitopes with variant numbers of GnRH peptide guided by a structural approach, we rationally engineered a CRM197 scaffolded multivalent immunocastration vaccine. Future studies are required to investigate the long-term immunological castration effects of TCG13 on other animals, and the immunization schedule should also be studied to achieve optimal efficacy.

Supplementary Information The online version contains supplementary material available at <https://doi.org/10.1007/s00253-024-13348-3>.

Author contribution This research was conceived and designed by ZW, YRD, and XWT. Experimental work was performed by YRD, WWC, and SL who also prepared and analyzed data. YRD designed the chimeric antigen sequences and produced all antigens for immunization. WRY provided adjuvant for vaccine preparation and contributed to the immunization protocol. YRD, MGL, SYT, WWC, and WJL extracted samples. YRD, JJZ, and JCW performed ELISAs. YRD led and completed animal experiment evaluations. ZW, YRD, and XWT wrote the manuscript. All authors read and approved the final manuscript.

Funding This research was supported by the Shandong Provincial Taishan Industry Leading Talent Project, China (tscy20170519).

Data availability All data generated and analyzed during this study are included in this published article and its supplementary information files.

Declarations

Ethics approval All the mice used in this research were maintained according to the local animal care guidelines in the Animal Care Unit of Qingdao University (approval numbers: No. 20220507BALB/c4020220823002, No. 20220921BALB/c3020230311003, and No. 20240808BALB/c1020240921011).

Conflict of interest The authors declare no competing interests.

Open Access This article is licensed under a Creative Commons Attribution-NonCommercial-NoDerivatives 4.0 International License, which permits any non-commercial use, sharing, distribution and reproduction in any medium or format, as long as you give appropriate credit to the original author(s) and the source, provide a link to the Creative Commons licence, and indicate if you modified the licensed material. You do not have permission under this licence to share adapted material derived from this article or parts of it. The images or other third party material in this article are included in the article's Creative Commons licence, unless indicated otherwise in a credit line to the material. If material is not included in the article's Creative Commons licence and your intended use is not permitted by statutory regulation or exceeds the permitted use, you will need to obtain permission directly from the copyright holder. To view a copy of this licence, visit <http://creativecommons.org/licenses/by-nc-nd/4.0/>.

References

- Alejandre J, Tildesley DJ, Chapela GA (1995) Molecular-dynamics simulation of the orthobaric densities and surface-tension of water. *J Chem Phys* 102(11):4574–4583. <https://doi.org/10.1063/1.469505>
- Azoitei ML, Ban YEA, Julien JP, Bryson S, Schroeter A, Kalyuzhnyi O, Porter JR, Adachi Y, Baker D, Pai EF, Schief WR (2012) Computational design of high-affinity epitope scaffolds by backbone grafting of a linear epitope. *J Mol Biol* 415(1):175–192. <https://doi.org/10.1016/j.jmb.2011.10.003>
- Bellone ML, Puglisi A, Dal Piaz F, Hochkoeppler A (2021) Production in *Escherichia coli* of recombinant COVID-19 spike protein fragments fused to CRM197. *Biochem Biophys Res Commun* 558:79–85. <https://doi.org/10.1016/j.bbrc.2021.04.056>
- Cao T, Zhang Z, Liu ZG, Dou X, Zhang J, Zhang W, Wu B, Yu ZD, Wei Z, Yu B (2016) High-level expression and purification of the major house dust mite allergen Der p 2 in *Escherichia coli*. *Protein Expres Purif* 121:97–102. <https://doi.org/10.1016/j.pep.2016.01.012>
- Chang AM, Chen CC, Hou DL, Ke GM, Lee JW (2021) Effects of a recombinant gonadotropin-releasing hormone vaccine on reproductive function in adult male ICR mice. *Vaccines (Basel)* 9(8):808. <https://doi.org/10.3390/vaccines9080808>
- Chang AM, Chen CC, Lee JW, Hou DL, Huang HH, Ke GM (2023) Effects of a novel recombinant gonadotropin-releasing hormone-1 vaccine on the reproductive function of mixed-breed dogs (*Canis familiaris*) in Taiwan. *Vaccine* 41(13):2214–2223. <https://doi.org/10.1016/j.vaccine.2023.02.061>
- Conde E, Bertrand R, Balbino B, Bonnefoy J, Stackowicz J, Caillot N, Colaone F, Hamdi S, Houmadi R, Loste A, Kamphuis JBJ, Huetz F, Guilleminault L, Gaudenzio N, Mougel A, Hardy D, Snouwaert JN, Koller BH, Serra V, Bruhns P, Grouard-Vogel G, Reber LL (2021) Dual vaccination against IL-4 and IL-13 protects against chronic allergic asthma in mice. *Nat Commun* 12(1):2574. <https://doi.org/10.1038/s41467-021-22834-5>
- Correia BE, Bates JT, Loomis RJ, Baneyx G, Carrico C, Jardine JG, Rupert P, Correnti C, Kalyuzhnyi O, Vittal V, Connell MJ, Stevens E, Schroeter A, Chen M, MacPherson S, Serra AM, Adachi Y, Holmes MA, Li YX, Klevit RE, Graham BS, Wyatt RT, Baker D, Strong RK, Crowe JE, Johnson PR, Schief WR (2014) Proof of principle for epitope-focused vaccine design. *Nature* 507(7491):201–206. <https://doi.org/10.1038/nature12966>
- Dalum I, Jensen MR, Gregorius K, Thomasen CM, Elsner HI, Mouritsen S (1997) Induction of cross-reactive antibodies against a self protein by immunization with a modified self protein containing a foreign T helper epitope. *Mol Immunol* 34(16–17):1113–1120. [https://doi.org/10.1016/s0161-5890\(97\)00147-8](https://doi.org/10.1016/s0161-5890(97)00147-8)
- De-Simone SG, Gomes LR, Napoleao-Pego P, Lechuga GC, de Pina JS, da Silva FR (2021) Epitope mapping of the diphtheria toxin and development of an ELISA-specific diagnostic assay. *Vaccines (basel)* 9(4):313. <https://doi.org/10.3390/vaccines9040313>
- Dunsha FR, Colantoni C, Howard K, McCauley I, Jackson P, Long KA, Lopaticki S, Nugent EA, Simons JA, Walker J, Hennessy DP (2001) Vaccination of boars with a GnRH vaccine (Improvac) eliminates boar taint and increases growth performance. *J Anim Sci* 79(10):2524–2535. <https://doi.org/10.2527/2001.79102524x>
- Einarsson S, Brunius C, Wallgren M, Lundström K, Andersson K, Zamaratskaia G, Rodriguez-Martinez H (2011) Effects of early vaccination with Improvac® on the development and function of reproductive organs of male pigs. *Anim Reprod Sci* 127(1–2):50–55. <https://doi.org/10.1016/j.anireprosci.2011.06.006>
- Fang F, Liu Y, Pu Y, Wang L, Wang S, Zhang X (2010) Immunogenicity of recombinant maltose-binding protein (MBP)-gonadotropin releasing hormone I (GnRH-I). *Syst Biol Reprod Med* 56(6):478–486. <https://doi.org/10.3109/19396368.2010.481005>
- Ferbitz L, Maier T, Patzelt H, Bukau B, Deuring E, Ban N (2004) Trigger factor in complex with the ribosome forms a molecular cradle for nascent proteins. *Nature* 431(7008):590–596. <https://doi.org/10.1038/nature02899>
- Ferro VA, Khan MAH, Earl ER, Harvey MJA, Colston A, Stimson WH (2002) Influence of carrier protein conjugation site and terminal modification of a GnRH-I peptide sequence in the development of a highly specific anti-fertility vaccine. Part i *Am J Reprod Immunol* 48(6):361–371. <https://doi.org/10.1034/j.1600-0897.2002.01120.x>
- Giannini G, Rappuoli R, Ratti G (1984) The amino-acid sequence of two non-toxic mutants of diphtheria toxin: CRM45 and CRM197. *Nucleic Acids Res* 12(10):4063–4069. <https://doi.org/10.1093/nar/12.10.4063>
- Gong XB, Yan X, Li MX, Di MY, Lu JT, Xu SS, Pan ZH, Zhu YY, Wu ZY, Zhang W, Qin P, Liu Y, Li YS, Fang FG (2024) Active immunization with recombinant GnRH6-CRM197 inhibits reproductive function of male rats. *Syst Biol Reprod Med* 70(1):131–138. <https://doi.org/10.1080/19396368.2024.2350372>
- Gupta SK, Minhas V (2017) Wildlife population management: are contraceptive vaccines a feasible proposition? *Front Biosci (Schol Ed)* 9(3):357–374. <https://doi.org/10.2741/s492>
- Hoffmann A, Bukau B, Kramer G (2010) Structure and function of the molecular chaperone trigger factor. *BBA-Mol Cell Res* 6:650–661. <https://doi.org/10.1016/j.bbamcr.2010.01.017>
- Jean-Paul Ryckaert GC, Berendsen HJC (1977) Numerical integration of the cartesian equations of motion of a system with constraints: molecular dynamics of n-alkanes. *J Comput Phys* 23:327–341. [https://doi.org/10.1016/0021-9991\(77\)90098-5](https://doi.org/10.1016/0021-9991(77)90098-5)
- Jiang SD, Hong MZ, Su SP, Song M, Tian Y, Cui P, Song S, Wang YY, Li FB, Fang FG (2015) Effect of active immunization against GnRH-I on the reproductive function in cat. *Anim Sci J* 86(8):747–754. <https://doi.org/10.1111/asj.12355>
- Khumsap S, Tangtrongsup S, Towiboon P, Somgird C (2024) GnRH vaccine could suppress serum testosterone in stallion mules. *Animals (Basel)* 14(12):1800. <https://doi.org/10.3390/ani14121800>
- Kim YH, Park BJ, Ahn HS, Han SH, Go HJ, Lee JB, Park SY, Song CS, Lee SW, Choi IS (2019) Immunocontraceptive effects in male rats vaccinated with gonadotropin-releasing hormone-I and -II protein complex. *J Microbiol Biotechnol* 29(4):658–664. <https://doi.org/10.4014/jmb.1901.01067>
- Lee TS, Cerutti DS, Mermelstein D, Lin C, LeGrand S, Giese TJ, Roitberg A, Case DA, Walker RC, York DM (2018) GPU-accelerated molecular dynamics and free energy methods in amber18: performance enhancements and new features. *J Chem Inf Model* 58(10):2043–2050. <https://doi.org/10.1021/acs.jcim.8b00462>
- Liu WL, Chen YH (2005) High epitope density in a single protein molecule significantly enhances antigenicity as well as immunogenicity: a novel strategy for modern vaccine development and a preliminary investigation about B cell discrimination of monomeric proteins. *Eur J Immunol* 35(2):505–514. <https://doi.org/10.1002/eji.200425749>
- Maier JA, Martinez C, Kasavajhala K, Wickstrom L, Hauser KE, Simmerling C (2015) ff14SB: Improving the accuracy of protein side chain and backbone parameters from ff99SB. *J Chem Theory Comput* 11(8):3696–3713. <https://doi.org/10.1021/acs.jctc.5b00255>
- Malito E, Bursulaya B, Chen CN, Lo Surdo P, Picchianti M, Balducci E, Biancucci M, Brock A, Berti F, Bottomley MJ, Nissum M, Costantino P, Rappuoli R, Spraggon G (2012) Structural basis for lack of toxicity of the diphtheria toxin mutant CRM197. *Proc Natl Acad Sci U S A* 109(14):5229–5234. <https://doi.org/10.1073/pnas.1201964109>

- Millar RP (2005) GnRHs and GnRH receptors. *Anim Reprod Sci* 88(1–2):5–28. <https://doi.org/10.1016/j.anireprosci.2005.05.032>
- Naz RK, Saver AE (2016) Immunocontraception for animals: current status and future perspective. *Am J Reprod Immunol* 75(4):426–439. <https://doi.org/10.1111/aji.12431>
- Ochoa JS, Favre RN, Garcia MF, Stornelli MC, Sangache WC, Rearte R, de la Sota L, Stornelli MA (2023) Immunocontraception of male domestic cats using GnRH vaccine Improvac. *Theriogenology* 198:211–216. <https://doi.org/10.1016/j.theriogenology.2022.12.020>
- Pichichero ME (2013) Protein carriers of conjugate vaccines characteristics, development, and clinical trials. *Hum Vaccin Immunother* 9(12):2505–2523. <https://doi.org/10.4161/hv.26109>
- Pöllabauer EM, Petermann R, Ehrlich HJ (2009) The influence of carrier protein on the immunogenicity of simultaneously administered conjugate vaccines in infants. *Vaccine* 27(11):1674–1679. <https://doi.org/10.1016/j.vaccine.2009.01.005>
- Pone EJ, Hernandez-Davies JE, Jan SR, Silzel E, Felgner PL, Davies DH (2022) Multimericity amplifies the synergy of BCR and TLR4 for B cell activation and antibody class switching. *Front Immunol* 13:882502. <https://doi.org/10.3389/fimmu.2022.882502>
- Siel D, Vidal S, Sevilla R, Paredes R, Carvallo F, Lapiere L, Maino M, Pérez O, Sáenz L (2016) Effectiveness of an immunocastration vaccine formulation to reduce the gonadal function in female and male mice by Th1/Th2 immune response. *Theriogenology* 86(6):1589–1598. <https://doi.org/10.1016/j.theriogenology.2016.05.019>
- Siel D, Huenchullán PR, Vidal S, Valdés A, Sáenz L (2024) Improving beef cattle production: safety and effectiveness of new immunocastration vaccine. *Animals (Basel)* 14(17):2538. <https://doi.org/10.3390/ani14172538>
- Ulker H, Yilmaz A, Karakus F, Yoruk M, Budag C, Deavila DM, Reeves JJ (2009) LHRH fusion protein immunization alters testicular development, ultrasonographic and histological appearance of ram testis. *Reprod Domest Anim* 44(4):593–599. <https://doi.org/10.1111/j.1439-0531.2007.01024.x>
- Vishweshwaraiah YL, Dokholyan NV (2022) Toward rational vaccine engineering. *Adv Drug Deliver Rev* 183:114–142. <https://doi.org/10.1016/j.addr.2022.114142>
- Wang C, Wang L, Chen BC, Yu H, Li L, Zhang KY, Yu B, Wei Z, Chen XF (2019) CRM197-coupled Der p 2 Peptides suppress allergic airway inflammation in a Der p 2-induced asthma mouse model. *Int Arch Allergy Imm* 180(3):173–181. <https://doi.org/10.1159/000502607>
- Wen Y, Jing YK, Yang L, Kang DQ, Jiang PP, Li N, Cheng JL, Li JW, Li XB, Peng ZC, Sun XZ, Miller H, Sui ZW, Gong Q, Ren BX, Yin W, Liu CH (2019) The regulators of BCR signaling during B cell activation. *Blood Sci* 1(2):119–129. <https://doi.org/10.1097/bs9.0000000000000026>
- Whitlock KE, Postlethwait J, Ewer J (2019) Neuroendocrinology of reproduction: Is gonadotropin-releasing hormone (GnRH) dispensable? *Front Neuroendocrinol* 53:100738. <https://doi.org/10.1016/j.yfrne.2019.02.002>
- Wu K, Minshull TC, Radford SE, Calabrese AN, Bardwell JCA (2022) Trigger factor both holds and folds its client proteins. *Nat Commun* 13(1):4126. <https://doi.org/10.1038/s41467-022-31767-6>
- Xu LL, Li ZJ, Su ZG, Yang YL, Ma GH, Yu R, Zhang SP (2019) Development of meningococcal polysaccharide conjugate vaccine that can elicit long-lasting and strong cellular immune response with hepatitis B core antigen virus-like particles as a novel carrier protein. *Vaccine* 37(7):956–964. <https://doi.org/10.1016/j.vaccine.2018.12.073>
- Zeigler DF, Gage E, Roque R, Clegg CH (2019) Epitope targeting with self-assembled peptide vaccines. *NPJ Vaccines* 4:30. <https://doi.org/10.1038/s41541-019-0125-5>

Publisher's Note Springer Nature remains neutral with regard to jurisdictional claims in published maps and institutional affiliations.